A Letters Journal Exploring the Frontiers of Physics

July 2008

EPL, **83** (2008) 28005 www.epljournal.org
doi: 10.1209/0295-5075/83/28005

Pattern of climate network blinking links follows El Niño events

A. Gozolchiani[1(a)], K. Yamasaki[2], O. Gazit[1] and S. Havlin[1]

[1] *Minerva Center and Department of Physics, Bar Ilan University - Ramat Gan, Israel*
[2] *Tokyo University of Information Sciences - Chiba, Japan*

received 2 May 2008; accepted in final form 2 June 2008
published online 3 July 2008

PACS 89.75.-k – Complex systems
PACS 92.10.am – El Niño Southern Oscillation
PACS 05.40.-a – Fluctuation phenomena, random processes, noise, and Brownian motion

Abstract – Using measurements of atmospheric temperatures, we create a weighted network in different regions on the globe. The weight of each link is composed of two numbers —the correlations strength between the two places and the time delay between them. A characterization of the different typical links that exist is presented. A surprising outcome of the analysis is a new dynamical quantity of link blinking that seems to be sensitive especially to El Niño even in geographical regimes outside the Pacific Ocean.

Introduction. – El Niño, a massive burst of heat exchange between the ocean and the atmosphere in the Pacific Ocean, is regularly tracked by measurements of sea surface temperatures and pressure differences in that zone [1]. When these measures reach a certain threshold level, the event begins. The end of the event is defined to be the time when the temperatures and pressures reach the threshold level again on their way to their base line [2]. This procedure cannot hold for other geographical zones that are also influenced. The reason is that in these zones the temperature fluctuations due to El Niño are of the same order as other fluctuations of temperature, due to other dynamical processes not related to El Niño. Another reason is that the pattern of an El-Niño–forced atmosphere is quite complex, yielding different qualitative and quantitative influences in different places (see, *e.g.*, [3]).

Here we show that by observing the pattern of climate network links we can follow El Niño events even in zones where the temperature does not show any effect.

The climate network is composed of nodes and links. The nodes are confined geographical zones that correspond to a single point of measurement on a grid. Each node carries a measured state variable that changes in time. The state variable in the current study is the temperature time series. A link between two nodes exists if there is a significant cross-correlation between their state variables' time series. A high peak in the cross-correlation function represents a strong link, and its position in time represents the time delay between the two nodes.

The distribution of the time delays is qualitatively similar everywhere around the globe. In every geographical zone studied there is always a small fraction of links between places whose temperatures oscillate coherently with very short time delays. There is a second, larger collection of pairs that exhibit intermediate correlation and change their time delays frequently. The third group is the group of pairs that show weak correlation. Our results suggest that mainly the last two groups modify their behavior in the presence of El Niño events (see fig. 1).

Using these general observations, we develop our analysis further by applying a symbolization approach to the time series composed of the cross-correlation values. The analysis exploits the highly increased sensitivity of correlation fluctuations to El Niño events, thus introducing a way to keep track of El Niño influences around the world.

Recent studies on climate networks [4,5] have identified differences in the climate network structure between El Niño and non–El-Niño time periods. Yamasaki *et al.* observed structural changes in the network. During El Niño many links disappear. Tsonis and Swanson divided their records into three parts —accumulation of all El Niño epochs, accumulation of all La Niña epochs and accumulation of the residual parts, and built a climate network based on temperature correlations from each part separately. They found differences in spatial distribution of links, yielding, on the whole, significantly less links in the El-Niño–based network. Our present study strongly supports refs. [4,5], adding detailed time-dependent information —the blinking of links during El Niño, which was missing.

(a) E-mail: avigoz@gmail.com

Table 1: Details on different geographical regions in the analyzed data.

Number of the region	Latitude	Number of points in the north-south direction	Longitude	Number of points in the east-west direction	Number of links
I	−30–30	9	120–285	23	21321
II	−30–30	9	0–105	14	7875
III	−90–(−60)	7	120–285	34	20910
IV	60–90	7	0–150	31	17391

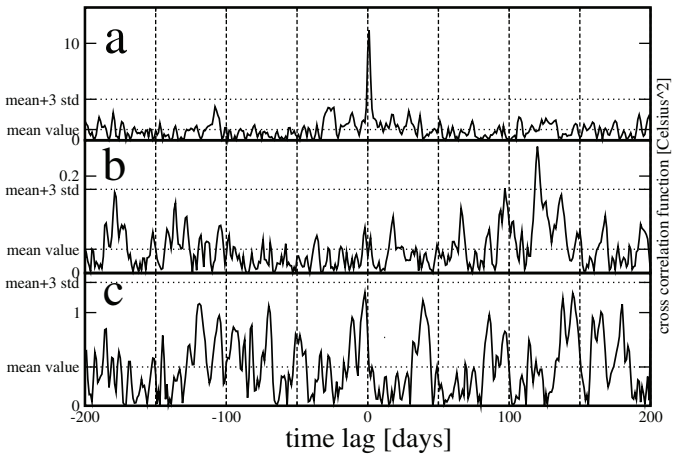

Fig. 1: Three typical profiles of the cross-correlation function of temperature anomalies (as defined in the text). The background values are of the order of the square value of the fluctuation of temperatures near the sea surface. (a) A strongly correlated (SC) link, with small time delay. (b) An intermediately correlated (IC) link, with a few significant time delays. (c) A weakly correlated (WC) link, where the different local maxima cannot be distinguished from noise.

The paper is organized as follows. In the first section we describe results that may be directly extracted from observations of the time behavior of the links between different places within different zones in the atmosphere. A new method, based on symbolic dynamics, is proposed in the second section. The outcome of this technique that successfully tracks the El Niño influence around the world is presented in the third section.

Observations. – We analyze daily temperature records arranged on a grid with a fixed latitude and longitude resolution throughout each zone between 5° and 7° for various geographical zones (see table 1)[1]. We filter out the annual trend, in order to get the anomaly daily temperature $T^y(d)$, where y is the beginning date of a year period, and d is the specific day in that specific period, ranging from 1 to 365. The range of y is between the beginning of the year 1979 and the beginning of the year 2005. Adjacent values of y differ by 50 days.

[1]These records are based on the analysis of a large collection of measurement databases using forecasting schemes. They are available in [6].

For each pair of sites in a specific zone z, we compute the absolute value of the cross-correlation function of temperatures. Figure 1 shows three typical examples of a cross-correlation function $X^y_{l,r}(\tau > 0) \equiv |\langle T^y_l(d) T^y_r(d+\tau)\rangle_d|$ and $X^y_{l,r}(\tau < 0) \equiv X^y_{r,l}(\tau > 0)$ between two temperature anomaly series indexed l, r. The strongly correlated links (SC) (fig. 1a) have usually a very dominant short time delay (between zero and three days) of coupling, which is clearly seen as a singled out peak much higher than the background of the cross-correlation function (at least 5 standard deviations). The intermediate correlated pairs (IC) (fig. 1b) have usually several time delays in which a more coherent motion may be observed. If there are both positive and negative dominant time delays, these pairs contribute to a long-term memory behavior. An event in one member of the pair influences the second member, and then shows back in the first member, completing the feedback loop. The weakly correlated pairs (WC) (fig. 1c) have many peaks in their cross-correlation function, which may be either due to noise, or due to some weak coupling. In WC links the maximal peak is of the order of the background.

We postulate that the SC links have the function of a skeleton that remains stable under the constant pressure of climate variability. Climate variability, which spans between very short time scales (specifically the scale of a few hours [7]) and longer periods (many days, and longer [1]) will consequently effect mainly IC links and WC links.

To support this assumption, we show (fig. 2a–c) the time delay of the most pronounced peak in the cross-correlation function of SCs, ICs, and WCs, as a function of the time index y. The time delays of SCs change in a very confined range between 0 and 3 days. They do not show significant sensitivity to climate variability. The ICs jitter between several partially stable time delays, in which they remain for some time, typically on the scale of several months. The WCs show a more rapid jitter between different time delays. This flexibility of the major mass of pairs (IC and WC) seems to become crucial for absorbing violent long-term patterns. As will be shown in the next section, it is possible to track El Niño (and most probably other climate variability patterns as well) by following massive changes that the non-skeleton pairs show.

This same structure may also be viewed through a scatter plot of time delays *vs.* correlation values (fig. 3).

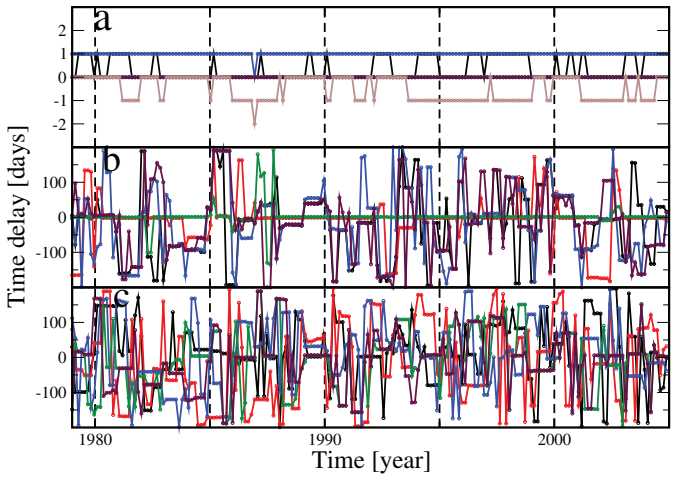

Fig. 2: (Colour on-line) Time delays of the highest value of the cross-correlation function as a function of the date y. (a) Five typical examples of SC links. (b) Five typical examples of IC links. (c) Five typical examples of WC links.

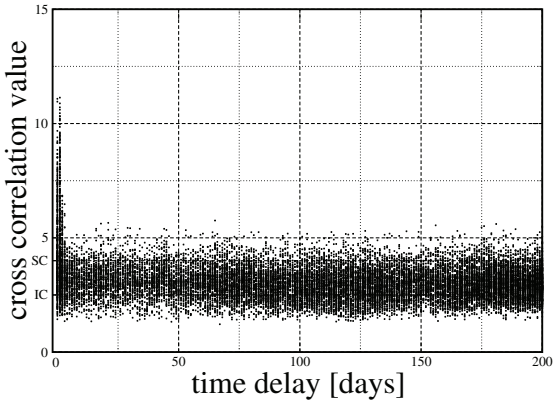

Fig. 3: Scatter plot of cross-correlation and time delays values. The ordinate grid-lines also include the ranges of the three groups. Below the line that is noted by IC is the range of WC links, above it and below the SC line is the range of IC links, and above the SC line only the strongest SC links exist.

The cross-correlation values (we shall also use the term *correlation strength*) are taken as the maximal value of $X^y_{l,r}(\tau)$ divided by its standard deviation. This choice efficiently distinguishes between the SC, IC, and WC links. In agreement with the previous discussion, SCs, with highest cross-correlation values, always have short time delays, while ICs and WCs have long-term relations. However, IC links have longer periods of a stable dominant time delay compared to WC links.

Method: symbolic dynamics of cross-correlations —blinking links. – Based on the findings in the previous section we present a simple method to study stability of links in the climate network that follows patterns related to El Niño, even far away from the El Niño basin.

We develop and apply symbolic time series analysis, a fruitful approach [8], which is believed to be sensitive to the nonlinearities of the dynamics [9]. In our case the time series is the time-dependent correlation strength of each link. We qualitatively explain in the next section the relation between certain nonlinear effects and the emergence of new symbols in the course of time.

The effects of El Niño events on the weak and the intermediate links has the form of fast attaching and de-attaching which we call *"blinking links"*. Setting a low threshold $H = 2$[STD] on the correlation strength enables us to observe clear sequences of links crossing the threshold whilst stable SC links (as well as other links that are not influenced) do not interfere.

In our method, a link with strength bigger (smaller) than H is now characterized by the number 1 (0). Thus, all links in the same zone and the same beginning date y yield a binary strength column $\vec{s}^z(y)$. We now group them in triples $\vec{S}^z_3(y) = \{\vec{s}^z(y), \vec{s}^z(y+1), \vec{s}^z(y+2)\}$. An element $\{\vec{S}^z_3(y)\}_\alpha$ of the triples column might have the values 111, 110, 101, 011, 100, 010, 001, 000, which are commonly denoted as symbols. The symbols 101 and 010 represent a situation where a certain link blinks, *i.e.* moves back and forth across the threshold H.

The sum of elements $b^z(y) = \sum_\alpha \delta(\{\vec{S}^z_3(y)\}_\alpha, \{1,0,1\}) + \sum_\alpha \delta(\{\vec{S}^z_3(y)\}_\alpha, \{0,1,0\})$, which is the number of blinking links, is a scalar function of time. The δ in the summand represents a generalized Kronecker delta for lists. As shown in fig. 4, the dynamics of $b^z(y)$ follow the El Niño events even far away from the El Niño basin. The less influenced zones show a weaker response, as expected.

While 101 and 010 patterns are relatively frequent in the presence of El Niño, higher-order blinking events that follow patterns of $\{\vec{S}^z_5(y)\}_\alpha$ (10101 and 01010), and even $\{\vec{S}^z_7(y)\}_\alpha$ (1010101 and 0101010) exist (see inset of fig. 4). These patterns are less likely to happen by chance, and therefore expected to yield a more clean indication of El Niño influence in places that are only weakly disturbed. However, they yield a much smaller fraction of the network, and therefore compose a poorly statistical measurement. This might be improved to some extent, if one begins with a more dense grid of measurement points.

Theory. – Next we suggest a theoretical explanation for the blinking phenomenon. A situation in which two nodes l and r are synchronized by a direct link that carries a strength $\epsilon_{l,r}$ and a time delay $\tau_{l,r}$ (with the direction from r to l) may be formally represented by two coupled differential equations for their phases:

$$\begin{aligned} \dot{\phi}_l &= X_l(\phi_l(t)) + \epsilon_{l,r} Y_{l,r}(\phi_l(t), \phi_r(t-\tau_{l,r})) + Z_l(t), \\ \dot{\phi}_r &= X_r(\phi_r(t)) + Z_r(t), \end{aligned} \tag{1}$$

where X_l is the autonomous dynamics of node l, $Y_{l,r}$ is the coupling function between the two nodes, and $Z_{l,r}(t)$ is the influence of the surrounding (other nodes, and external noise). Such a system (as well as the more general case of bi-directional coupled systems) might exhibit "generalized

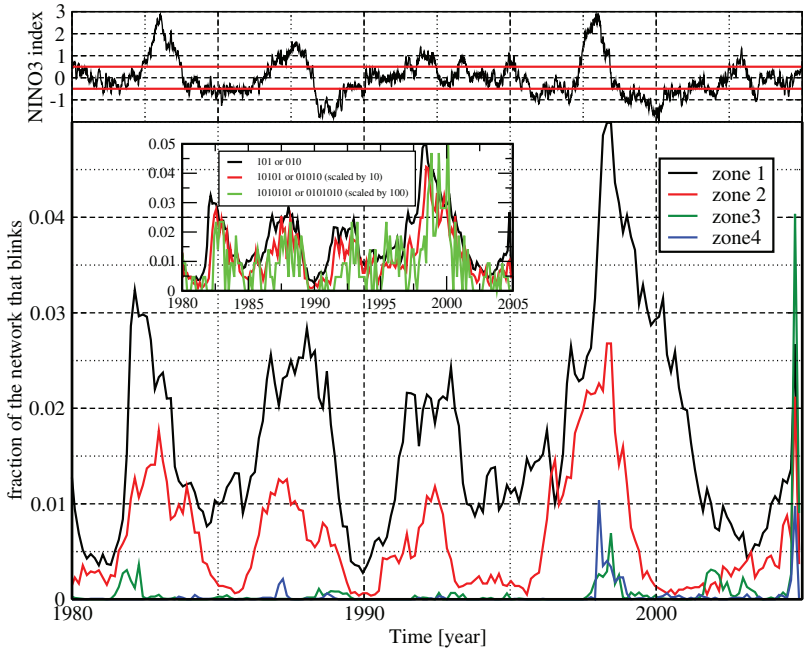

Fig. 4: (Colour on-line) Upper panel : the NINO3 index, composed of sea surface temperature in the Pacific Ocean. The red lines are accepted threshold values [2]. Lower panel : number of blinking links $b^z(y) = \sum_\alpha \{\vec{S}_3^z(y)\}_\alpha$ as a function of the time y. The inset shows higher-order blinking patterns for zone 1. The 5th-order fractions are scaled by 10 and the 7th-order fractions are scaled by 100.

synchronization" under certain conditions [10,11], thus yielding a delayed correlated motion of ϕ_l and ϕ_r.

It has nevertheless been noted that such a correlation might result from a spurious causality relation caused by a latent node [12] that influences both ϕ_l and ϕ_r. There is a third option, that the causality relation between the two nodes is indeed real, but the underlying relation goes through one or more indirect paths [12,13]. In the last two cases, dropping of links in the indirect path is observed as changes of the correlation of ϕ_l and ϕ_r.

If there is only one indirect path, and no direct paths, breaking of links lying on that path will obviously destroy correlations between ϕ_l and ϕ_r. If there is more than one path, and each of the indirect paths carries a different set of time delays and coupling strengths, destroying some of the indirect paths not necessarily cause lower correlations between ϕ_l and ϕ_r, because the different paths might be interfering.

The effective situation is similar to the one that will be observed in the following dynamics:

$$\begin{aligned} \dot{\phi}_l &= X_l(\phi_l(t)) + \textstyle\sum_i \epsilon^i_{l,r} Y^i_{l,r}(\phi_l(t), \phi_r(t - \tau^i_{l,r})) + Z_l(t), \\ \dot{\phi}_r &= X_r(\phi_r(t)) + Z_r(t), \end{aligned} \tag{2}$$

where the index i distinguishes between the latent indirect paths. A process of breaking links in the network causes lower correlations between the directly linked nodes. However, *most* of the pairs are related by indirect relations of the form of eq. (2). In these cases the change of the coupling strengths $\epsilon^i_{l,r}$ does not cause just a mere drop of the correlation, but instead, it causes instability which is indeed observed as *blinks* (as seen on fig. 4). Therefore, the nonlinear pattern that symbolization tracks in the case of the climate network might be related to a break of intermediate competing paths. The main point is that blinking is expected to be the most dramatic effect of breaking of links, rather than the complete break of correlation that is expected to show only between directly coupled pairs.

Summary. – We have designed in the current work a tool that enables to follow the influence of El Niño on the atmosphere in different geographical zones. The method relies on the understanding that temperature anomalies of two places that are moderately correlated (IC links) hold a rich multi-time-delayed dynamics, while highly correlated links compose a skeleton that does not respond to El Niño. We have shown that the dynamics of the dominant time delay between two geographical regions is fundamentally different among the different classes of correlation strength.

The essence of the method lies in the application of symbolization to the strength of the links. For this purpose we have chosen a class of symbols that represent blinking links, *i.e.*, a complete instability of a link. Other symbols also hold information, and classifying them is a challenge that we plan to issue in a future work.

When local changes occur in a network, many pairs of nodes which do not directly belong to the basin of the extreme event also feel the change. Because of delayed feedbacks, changes in the form of breaking of links in a restricted zone can either increase or decrease the

correlations between the pairs which were not affected directly by the initial perturbation. We have suggested that blinking is related to indirect influence of breaking of links in a restricted region in the network. This general concept may provide a way to follow the propagation of large perturbations in the atmosphere.

* * *

We wish to thank Prof. S. Brenner and Prof. H. Von Storch for useful discussions. We also thank the EU project DAPHNet, ONR, the Israel Science Foundation, Frontier project of Tokyo University of Information Sciences, Hadar Foundation and the Israel Center of Complexity Science for financial support.

REFERENCES

[1] Dijkstra H. A., *Nonlinear Physical Oceanography* (Kluwer Academic Publishers) 2000.
[2] Trenberth K. E., *Bull. Am. Meteorol. Soc.*, **78** (1997) 2771.
[3] `http://www.ncdc.noaa.gov/paleo/ctl/clisci10c.html`.
[4] Yamasaki K., Gozolchiani A. and Havlin S., *Phys. Rev. Lett.*, **100** (2008) 228501.
[5] Tsonis A. A. and Swanson K. L., *Phys. Rev. Lett.*, **100** (2008) 228502.
[6] `http://www.cdc.noaa.gov`. NCEP Reanalysis data, NOAA/OAR/ESRL PSD, Boulder, Colorado, USA.
[7] Tsonis A. A. and Elsner J. B., *Nature*, **333** (1988) 545.
[8] Daw C. S., *Rev. Sci. Instrum.*, **74** (2003) 915.
[9] Ashkenazy Y., Ivanov P. Ch., Havlin S., Peng C.-K., Goldberger A. L. and Stanley H. E., *Phys. Rev. Lett.*, **86** (2001) 1900.
[10] Kocarev L. and Parlitz U., *Phys. Rev. Lett.*, **76** (1995) 1816.
[11] Pikovsky A., Rosenblum M. and Kurths J., *Synchronization: A Universal Concept in Nonlinear Sciences* (Cambridge University Press) 2001.
[12] Eichler M., *Philos. Trans. R. Soc. B*, **360** (2005) 953.
[13] Schelter B., Winterhalder M., Dahlhaus R., Kurths J. and Timmer J., *Phys. Rev. Lett.*, **96** (2006) 208103.